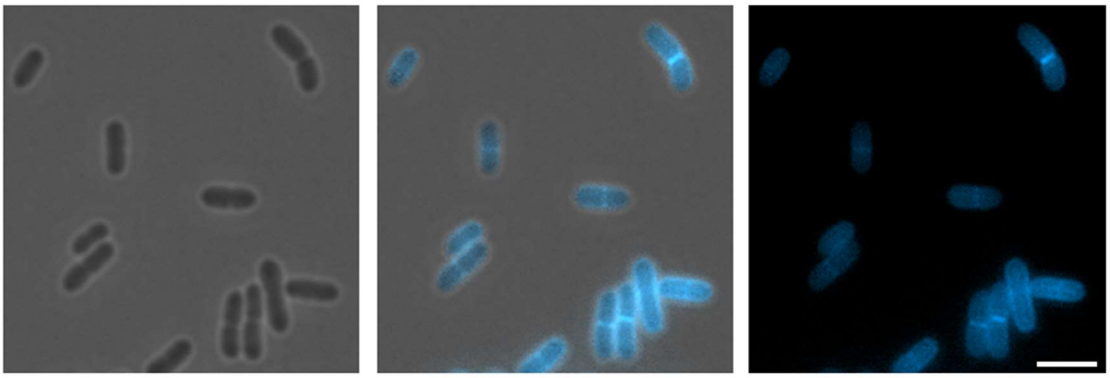

Figure S1. Growing sites of Zm6 cells visualized by a HADA-labeling. Zm6 cells growing under anaerobic conditions were stained with HADA at 500 μM for 30 minutes under a dark condition. The cells were then washed with PBS twice and mounted on PBS agarose pad and imaged by a fluorescence microscope. The labeling showed that *Z. mobilis* cell incorporated new cell wall materials at its division site and lateral walls. Left panel; a phase contrast image. Middle; an overlay of phase contrast and fluorescence images. Right; a fluorescence image. Blue; HADA. Scale bar; 4 μm.

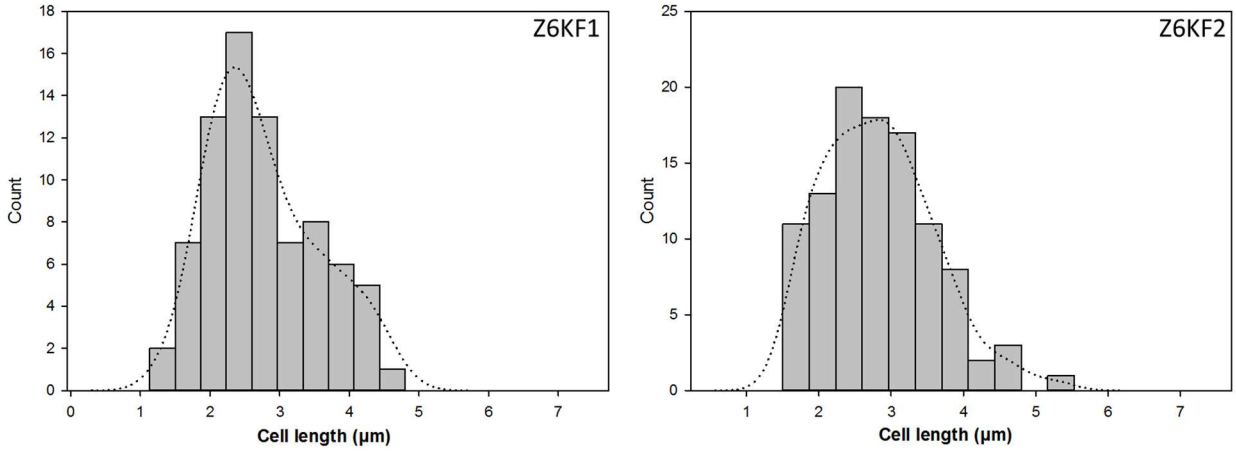

Figure S2. Histogram and Kernel density plot of cell length in growing *Z. mobilis* strains Z6KF1 and Z6KF2. Growing Z6KF1 (OD_{600} 0.8) and Z6KF2 (OD_{600} 0.32) culture was directly mounted on PBS agarose pad and imaged by phase contrast microscopy. The mean of cell length was 2.78 μm for Z6KF1 (*n* = 79) and 2.83 μm for Z6KF2 (*n* = 104). The bandwidth used for the Kernel density plot was 0.299 for Z6KF1 and 0.272 for Z6KF2. To test the functionality of FtsZ-GFP fusion protein, we first examined if the expression altered morphology or cell size in the strain Z6KF2. Despite that overexpression of *ftsZ* is known to cause reduction of cell size in several bacteria, the cells did not show any obvious morphological changes. The result suggested two possibilities; an overexpression of functional FtsZ-GFP did not alter cell function in the strain, or that the fusion protein was not functional and did not cause any dominant negative effects. The strain Z6KF1 carrying intact *ftsZ* in the pBBR plasmid, exhibited no obvious morphological defects either, indicating that overproduction of functional FtsZ by the pBBR1 plasmid was not overwhelming the native production of Zm6 FtsZ. Note that same upstream promoter was used for expressions of *ftsZ* in Z6KF1 and *ftsZ-GFP* in Z6KF2. These phenotypic observations, together with subcellular localization of the *Z. mobilis* FtsZ-GFP fusion

in the strain Z6KF2, indicated that FtsZ-GFP did not cause much disturbance to the cellular organization in the expressed strain.

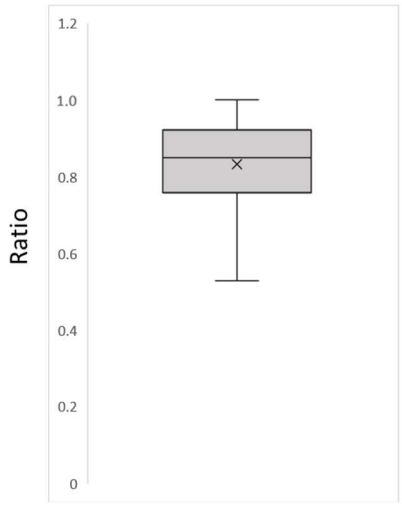

Figure S3. Box and whisker plot of ratio of short:long cell compartment length in growing *Z. mobilis* strains Z6KF2. Cell compartment length was defined as distance between a cell pole to Z-ring position. The box shows the ratio of short:long cell-compartments. The box is marked with mean (x) and median (middle line of the box). Note that the mean value of the cell compartment ratio (0.833) is very close to the ratio of dividing daughter cells (0.837) in the Figure 1, showing that Z-ring positions represent division sites in *Z. mobilis* cells. *n* = 106.

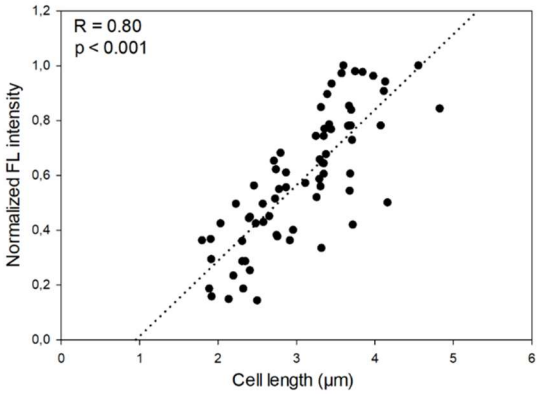

Figure S4. Plot of normalized FtsZ-GFP peak intensity within a cell by a function of its cell length. The linear relationship indicates that cells accumulated FtsZ ring linearly along with cell growth. Perason's r = 0.8, p-value < 0.001. *n* = 80.

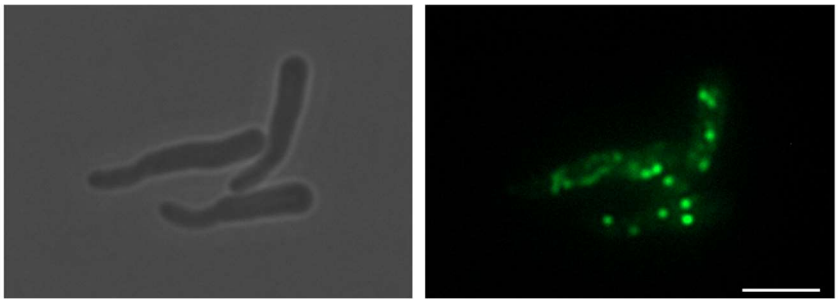

Figure S5. FtsZ-GFP sub-cellular localizations in salt stress-induced filamentous Z6KF2 cells. The Z6KF2 culture was grown in the complex medium supplemented with 0.2 M NaCl. The growing filamented cells were directly mounted on agarose pad of the identical growth medium, and fluorescence imaging was performed. FtsZ-GFP formed either foci or filamentous structured in the elongated cells. Left; phase contrast image. Right; fluorescence image. Green; FtsZ-GFP. Scale bar; 5 μm.

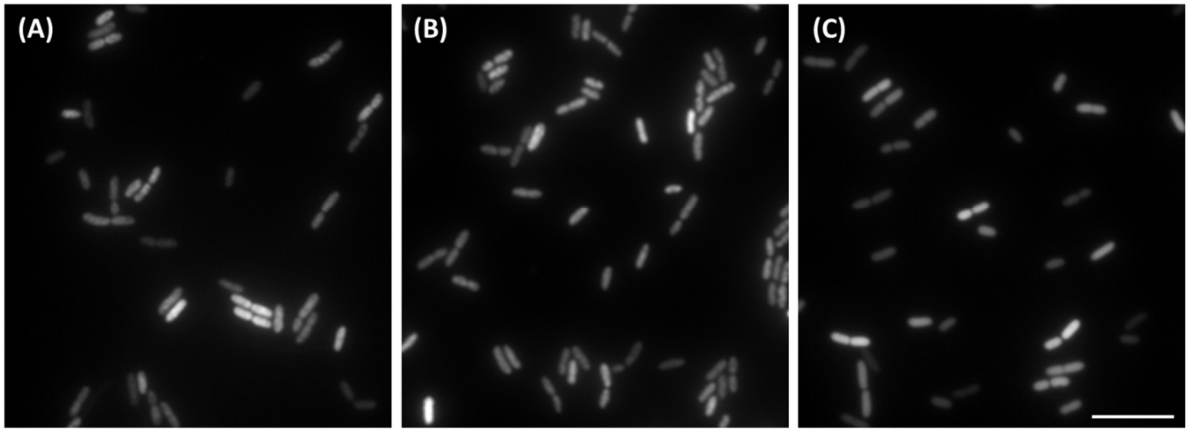

Figure S6. Visualizing *Z. mobilis* nucleoids by different staining methods. The staining was to examine if variant FL signal intensities found in Zm6 cells (Fig. 5A, 5C) were due to possible artifacts from the staining procedure. (A) Growing Zm6 cells stained with DAPI 50 µg/ml for 20 minutes. (B) Growing Zm6 cells stained with SYTO 9 at 11 µM for 10 minutes. (C) SYTO 9 staining of chemically fixed Zm6 cell. The cells were fixed by 10% formalin (v/v) for half hour, washed with PBS and stained with SYTO 9 at 0.5 µM. The cells were washed with PBS in all tested methods before imaging. All three staining procedures resulted in the variant FL signal intensities between Zm6 cells. The result of (A) ruled out a possibility of dye-specific artefact as a cause of the variant FL signals among individual Zm6 cells. The result of (B) excluded a possibility of artefact caused by a depletion of dye in (Fig. 5A). The result of (C) excluded a possibility of stress-response based phenomenon to cause the variant FL intensities in (Fig. 5A). White; fluorescence signals from the dyes. Scale bar; 10 µm.

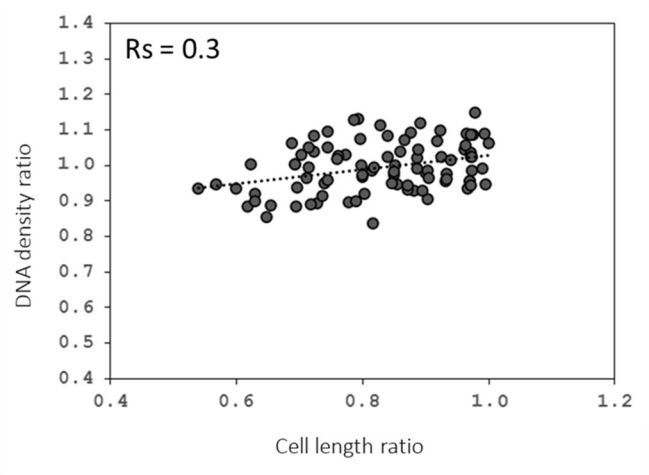

Figure S7. Plot of cell DNA crowdedness ratio by a function of ratio of cell length between paired-sibling cells (short:long cell length). DNA crowdedness/density was an average of FL signal intensities within cell. Spearman's rank correlation test; Rs = 0.3, p-value > 0.001, *n* = 90.

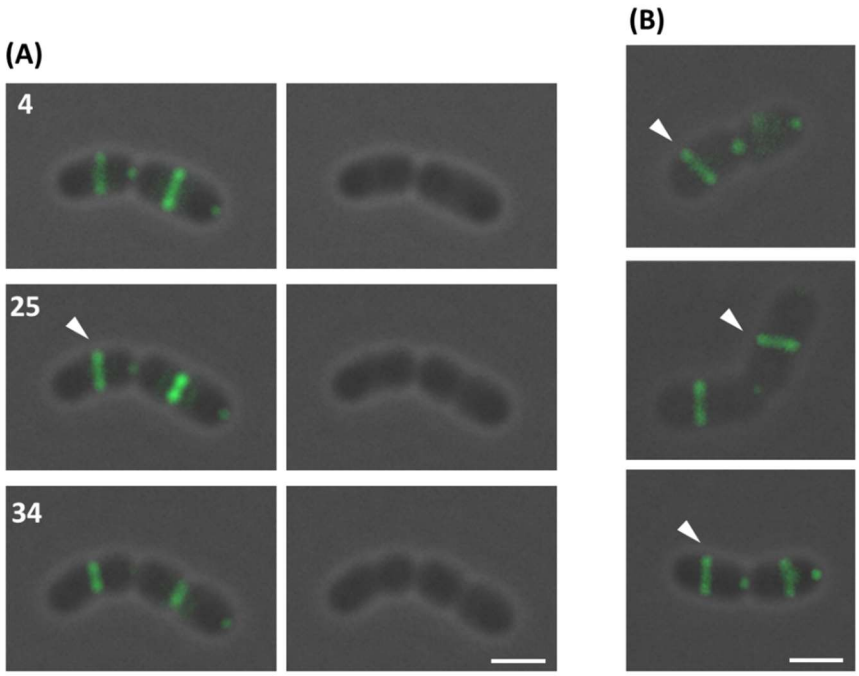

Figure S8. Inclined Z-rings in Z6KF2 cells. (A) Short time-lapse imaging of Z6KF2 cells anaerobically growing on the complex medium agarose pad. Left panels, overlays of phase contrast and fluorescence images (green: FtsZ-GFP). Right panels, phase contrast images. Numbers indicate minutes after imaging started. (B) Single time imaging of growing Z6KF2 cells. Images are overlays of phase contrast and fluorescence images. Note that Z-rings were leaned from the short axis in some of growing Z6KF2 cells. White arrowheads indicate inclined Z-ring in all images. Scale bars; 2 μm for all images.

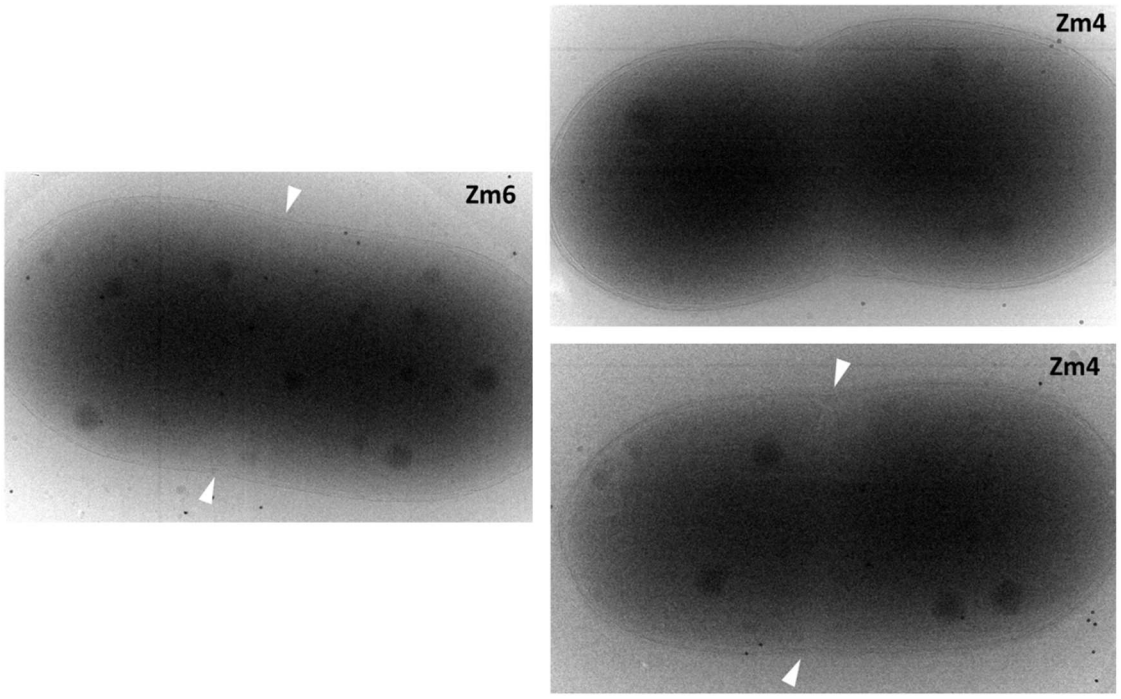

Figure S9. Electron micrographs of the strain Zm6 cell (left) and the strain Zm4 cells (right). Arrowheads indicate constriction sites that are slightly inclined from short vertical axis of cells.